PKU-TP-98-31
hep-ph/9807533
July 1998

Demonstration of the double Q^2-rescaling model

Hong-an Peng[1,2], Cong-feng Qiao[2], Jia-sheng Xu[1], and Zhen-min He[2,3]
1. *Department of Physics, Peking University, Beijing 100871, P.R. China*
2. *CCAST (World Laboratory), P.O.Box 8730, Beijing 100080, P.R. China*
3. *Department of Physics, HeBei Teachers' University, Shijiazhuang, 050016, P.R. China*

arXiv:hep-ph/9807533v1 29 Jul 1998

Abstract

In this paper we have demonstrated the double Q^2-rescaling model (DQ^2RM) of parton distribution functions of nucleon bounded in nucleus. With different x-region of l-A deep inelastic scattering process we take different approach: in high x-region ($0.1 \leq x \leq 0.7$) we use the distorted QCD vacuum model which resulted from topologically multi-connected domain vacuum structure of nucleus; in low x-region ($10^{-4} \leq x \leq 10^{-3}$) we adopt the Glauber (Mueller) multi-scattering formula for gluon coherently rescattering in nucleus. From these two approach we justified the rescaling parton distribution functions in bound nucleon are in agreement well with those we got from DQ^2RM, thus the validity for this phenomenologically model are demonstrated.

PACS number(s): 12.39.Ba, 12.90.+b, 24.85.+p

Typeset using REVTEX

I. INTRODUCTION

Deeply understanding the parton distribution functions (PDF) of the nucleon bounded in nucleus are very important both for studying particle and high-energy nuclear physics. Since the middle of eighties many important progress has been achieved both from experimental and theoretical studies [1]. It has revealed experimentally that the PDF of a bound nucleon has remarkable difference from that of a free one: the EMC effect in high x-region ($0.1 \leq x \leq 0.7$) [2] and the nuclear shadowing effect [3] in low x-region ($x \leq 10^2$) are the most important examples. Of the EMC effect, many models have been proposed [1,4], all of them could more or less explain the relevant data, but for the nuclear shadowing effect only the constituent quark Q^2-rescaling model and the extended x-rescaling model can make out satisfactory explanations after introducing some shadowing parameters [1,5]. As far as we know none of these models could describe the PDF of a bound nucleon which cover both the available kinetic x and Q^2 range and could explained well all the data from high energy l-A and h-A basic processes. Of course building such a model is very difficult, but is also very needed. We have tried to take this task and proposed from phenomenology the double Q^2-rescaling model (DQ^{2}RS) [6], from which the calculated results agree rather well with experimentally relevant data.

In this paper we want to demonstrate our DQ^{2}RM from physical observations. We take different approach at different x-region of l-A DIS. In high x-regions (according EMC effect which means ($0.1 \leq x \leq 0.7$), for fixed Q^2, it should correspond relatively low energy region so the non-perturbative QCD effects would be important in this x-region. We observe the QCD vacuum around the bound nucleon is modified topologically by multi-connected domain vacuum structure of the nucleus. We further use soliton bag model of Lee *et al* [7] and find the radius of a nucleon bounded in nucleus with nucleon number A is larger than that of a free one, $r_A > r_N$ [8]. According to uncertainty principle, the PDF of a bound nucleon would then be soften in comparison with that of a free one and shift the PDF to small x side, which are consistent with those from DQ^{2}RM, thus we demonstrated our model at high x-region. In low x-region which covered by available data ($10^{-4} \leq x \leq 10^{-3}$), it is well known the gluon distribution predominated in PDF of a nucleus and the coherent interaction of gluons from neighbour nucleons with same impact parameter in a nucleus becomes important. Following the method of Levin *et al* [9], we adopt the Glauber (Mueller) [10] multi-scattering formula for calculating contributions of gluon coherently rescattering in nucleus, thus we get the gluon distribution function of the nucleon bounded in any nucleus (A) and find it agree well with those from DQ^{2}RM.

The organic of this paper is as follows: in sec. II we recapitulate the DQ^{2}RM and its relatives. A detail demonstration on DQ^{2}RM both for high and low x-region will be given respectively in sec.III and sec. IV. The last sec V is the conclusion and some comments.

II. RECAPITULATION OF DQ^{2}RM

Since nuclei are formed from weakly bounded nucleons, one could expected the basic properties of the nucleon in nucleus, including the behavior of parton distribution, are not far from that of the free nucleon. All nuclear effects revealed in l-A DIS should be attributed to this nuclear environment which comes from the weakly bounding mechanism. According to this observation and informations from relevant phenomenology, we proposed in [6] the following relations of PDF between bounded and free nucleon:

$$\begin{aligned} q_{V_i}^A(x,Q^2) &= q_{V_i}^N(x,\xi_V^A Q^2), \quad (i=u,d,s) \\ q_{S_i}^A(x,Q^2) &= \bar{q}_{S_i}^A(x,Q^2) = q_{S_i}^N(x,\xi_S^A Q^2), \\ g^A(x,Q^2) &= g^N(x,\xi_g^A Q^2), \end{aligned} \tag{1}$$

where rescaling parameter's $\xi_\alpha^A(\alpha = V,S,g)$ are depending on and very slowly increased with nucleon number A.

Since it must respect total momentum conservation,

$$\int_0^1 x dx \left\{ \sum_i [q_{V_i}^A(x,Q^2) + q_{S_i}^A(x,Q^2) + \bar{q}_{S_i}^A(x,Q^2)] + g^A(x,Q^2) \right\} = 1. \tag{2}$$

Only two among $\xi_\alpha^A(\alpha = V,S,g)$ are independent, so this model is called the double Q^2-rescaling model.

At present the statistics and the precision of experimental data on relevant processes are insufficient to test very precisely theoretical calculation, so in our calculation only the leading order approximation on the formulas of hard subprocesses and parton distribution functions are considered. Thus in DQ^{2}RM the structure function and gluon distribution function of bound nucleon respectively is

$$F_2^A(x,Q^2) = \sum_i e_i^2 x \left\{ q_{V_i}^N(x,\xi_V^A Q^2) + q_{S_i}^N(x,\xi_S^A Q^2) + \bar{q}_{S_i}^N(x,\xi_S^A Q^2) \right\} \tag{3}$$

$$x g^A(x,Q^2) = x g^N(x,\xi_g^A Q^2). \tag{4}$$

$F_2^A(x,Q^2)$ denotes the average nucleon structure function of an ideal nucleus with $N = Z = \frac{1}{2}A$.

The nuclear effect of nucleon structure functioned and the gluon distribution may be represented by following ratios

$$R^{A/D}(x,Q^2) = F_2^A(x,Q^2)/F_2^D(x,Q^2), \tag{5}$$

$$R_g^{A/D}(x,Q^2) = g^A(x,Q^2)/g^D(x,Q^2), \tag{6}$$

For the Drell-Yan process in p-A collision the nuclear effect is represented by the ratio

$$T^{A/N} = \int \frac{d^2\sigma^{p-A}(x,x_t,Q^2)}{dxdx_t}dx / \int \frac{d^2\sigma^{p-N}(x,x_t,Q^2)}{dxdx_t}dx, \tag{7}$$

where

$$\frac{d^2\sigma^{p-A(N)}(x,x_t,Q^2)}{dxdx_t} = \frac{1}{3}\frac{4\pi\alpha^2}{3m_{l\bar{l}}^2}\sum_i e_i^2 \left\{ \left[q_{V_i}^p(x,Q^2) + q_{S_i}^p(x,Q^2) \right] \bar{q}_{S_i}^{A(N)}(x_t,Q^2) + \bar{q}_{S_i}^p(x,Q^2) \left[q_{V_i}^{A(N)}(x_t,Q^2) + q_{S_i}^{A(N)}(x_t,Q^2) \right] \right\}, \tag{8}$$

Three parameters $\xi_\alpha^A(\alpha = V,S,g)$ in DQ^{2}RM are determined as follows: firstly we choose suitable ξ_V^A and ξ_S^A to explain the nuclear effect in l-A DIS process Eq.(5); secondly we describe p-A Drell-Yan process with Eq.(7) and finally determine ξ_g^A by using nuclear momentum conservation Eq.(2) and explain the nuclear effect of γ^*-A electroproduction J/ψ process in Eq.(6).

We adopted the PDF of free nucleon given by Gluck- Reya- Vogt (GRV) [11] because this formalism allows to be evoluted inversely to $Q^2 \leq 1$ GeV^2, this is quite important point for getting the PDF of sea quark and gluon of bound nucleon by Eq.(1) at $\xi_S^A < 1$ and $\xi_g^A < 1$.

The Q^2-rescaling parameters ξ_V^A, ξ_S^A and ξ_g^A on nuclei C^{12}, Ca^{40}, Fe^{56} and Sn^{119} obtained by above method from the data of references [3,12–14] are listed in Table 1[1]. It is worth to note that all of ξ_V^A and large than unity and increased slowly with A, but all of ξ_S^A and ξ_g^A are smaller than unity and decreased slowly as A increasing.

Using the parameter listed in Table 1 and relevant Eqs. (1)-(8), together with GRV parametrization for PDF of free nucleon, the theoretical predications on $R^{A/D}(x,Q^2), T^{A/N}(x,Q^2)$ and $R_g^{A/D}(x,Q^2)$ for nuclei C^{12}, Ca^{40}, Fe^{56} and Sn^{119} by DQ^{2}RM could be obtained.

---

[1]In ref. [6] the Q^2-rescaling constants of Sn^{119} which we have fitted are $\xi_V^{Sn} = 1.57$, $\xi_S^{Sn} = 0.45$ and $\xi_V^{Sn} = 0.58$, but after recalculating we find it is better to take these values shown in Table I instead.

The results calculated from DQ^{2}RM in ref. [6] as follows: 1. The curves of $R^{A/D}(x.Q^2)$ on l-A DIS processes for nuclei C^{12}, Ca^{40}, Fe^{56} and Sn^{119} within Q^2 range given in [3,12] are separatedly plotted in Fig.1(a-d) where corresponding experimental data [3,12] are shown. 2. The curves of $T^{A/D}(x, Q^2)$ on p-A Drell-Yan process for nuclei C^{12}, Ca^{40} and Fe^{56} within region of $0.025 \leq x \leq 0.30$, $4 \leq m_{l\bar{l}} \leq 9$ GeV and $E_{CM} = 40$ GeV are separately plotted in Fig.2(a-c), where corresponding experimental data [13] are shown. 3. The curves of $R_g^{Sn/C}(x, Q^2)$ (the ratio of gluon distribution function of nucleus Sn to that of nucleus C) is plotted in Fig.3 where the experimental data [14] of the ratio measured in $\gamma^* + A \to J/\psi + X$ process are shown.

For comparison we have also plotted in Fig.1-3 the corresponding curves which calculated from original single Q^2-rescaling model (as pointed by Li *et al* in [15]. This model with a common Q^2-rescaling parameter $\xi(A)$ for valance quark, sea quark and gluon, leads to non-conservation of nuclear momentum).

From above illustration, we can see that by using DQ^{2}RM all calculated ratios, which representing the nuclear effects on PDF of bound nucleon, agree rather well with that from relevant experimental data, Since the essential elements of this model are embodied in Table 1. we shall demonstrate it in following sections.

III. DEMONSTRATION FOR DQ^{2}RM IN HIGH X-REGION

In l-A(N) DIS process the Bjorken variable $x = \frac{Q^2}{\hat{S}+Q^2}$, where $\hat{S}$ is the square of center-mass energy of γ^* and scattered nucleon. For fixed Q^2, the higher x region correspond to lower energy region. Thus in high x-region ($0.1 \leq x \leq 0.7$) the non-perturbative QCD effects should be important and the behavior of PDF of the nucleon should depends on space-time property of hadron environment. In the following we will use the soliton bag model of T.D. Lee [7] to justify the QCD vacuum structure of a bound nucleon is topologically different from that of a free one (an isolated nucleon). The consequence of this difference is the radius of bound nucleon would be large than that of free one. i.e. $r_A > r_N$. Thus, in comparing with free nucleon, the PDF of bound nucleon shift to its small x end.

comparing QCD with QED and introducing the concept of colour dielectric constant κ, Lee found that the vacuum polarization of QCD shows a colour anti-screening property. On account of this a phenomenological scalar field $\sigma(x)$ is introduced into Lagrangian $\mathcal{L}$ of Lee's model to describe the colour dielectric property of vacuum. This $\sigma(x)$ is treated as a classical field with an effective potential shown in Fig.(4). The potential energy $V(\sigma)$ has an absolute minimum $V(\sigma_{vac}) = 0$ at $\sigma = \sigma_{vac}$. which represent the QCD physical vacuum out of the

nucleon bag and which correspond to a complete colour antiscreening with $\kappa = 0$. Inside the bag there are QCD perturbative vacuum around the colour quarks, where the field $\sigma = 0$ and correspond to $\kappa = 1$.

In the case of nucleus, since many nucleons densely populated, the physical QCD vacuum out of any nucleon which bagged by the nucleus is a multi-connected domain and so it has a different topologically vacuum structure comparing with that of free one (isolated nucleon) which is a single-connected domain. In terms of Lee model which means, for a nucleon with A nucleons, the σ field in the domain occupied by the remainder (A-1) bags has a value $\sigma = 0(\kappa = 1)$ instead of $\sigma = \sigma_{vac}(\kappa = 0)$. On the average, the effective QCD physical vacuum out of bound nucleon bag correspond to scalar field σ_A (the relevant vacuum colour dielectric constant κ_A) which must smaller than σ_{vac}, the difference $(\sigma_{vac} - \sigma_A)$ increase with increasing of A. From Fig.4. one could see, comparing with isolated bag where the vacuum pressure on its surface is B and its equilibrium radius is r_N, the bound nucleon bags would bear smaller vacuum pressure B_A $(B_A < B)$ and enlarge equilibrium bag radius $r_A(r_A > r_N)$. To estimate ΔB_A, a liner relation between σ and κ assumed as in Lee model,

$$\sigma_A = \sigma_{vac}(1 - \kappa_A) \tag{9}$$

expand $V(\sigma_A)$ closely around σ_{vac} and take the first non-zero term,

$$V(\sigma_A) = b(\sigma_A - \sigma_{vac})^2 \tag{10}$$

where $b > 0$ according to the definition of physical vacuum. Expressing σ_A by Eq.(9) we get

$$\Delta B_A = b\sigma_{vac}^2 \kappa_A^2 \equiv G\kappa_A^2 \tag{11}$$

A simple and intuitive method estimating the effective constant κ_A is to consider the volume ratio which the nucleus occupied with that of (A-1) surrounding nucleons. From geometry picture consideration we get

$$\kappa_A = \frac{A^\alpha - 1}{\frac{3A^\alpha}{4\pi\rho_A r_A^3} - 1} \tag{12}$$

where ρ_A is the nucleon number density in the nucleus A. In order to avoid overestimating the effect of those bags far away from the considered nucleon a parameter $\alpha \leq 1$ is introduced and we find $\frac{1}{3} \leq \alpha \leq \frac{2}{3}$ are reasonable values.

The relation between ΔB_A and r_A is determined by Eqs.(11) and (12). On the other hand the equilibrium condition of the pressures inside and outside of the bag is determined by the formula of the bag model [16]

$$M = \frac{C}{r} + \frac{4\pi}{3} r^3 B \tag{13}$$

where $c = 3\epsilon - \alpha_c \sum_{i,j} (\sigma_i \sigma_j)(\lambda_i^a \lambda_j^a)$ $\not{h} - Z_0$ is constant in our case, from Eq.(13) we can induce to another relation between ΔB_A and r_A:

$$\Delta B_A = \frac{3 M_N r_N}{16\pi} (\frac{1}{r_N^4} - \frac{1}{r_A^4}) \tag{14}$$

M_N is the mass of a free nucleon. Combining Eqs.(11), (12) and (14) we can obtain the self-consistent equation for determining the nucleon bag radius, r_A, in the nucleus;

$$G(\frac{A^\alpha - 1}{\frac{3A^\alpha}{4\pi\rho_A r_A^3} - 1})^2 = \frac{3 M_N r_N}{16\pi} (\frac{1}{r_N^4} - \frac{1}{r_A^4}) \tag{15}$$

since $G \equiv b\sigma_{\rm vac}^2 > 0$, Eq.(15) shows $r_A > r_N$.

After the EMC effect discovered experimentally, Jaffe and Close *et al* [4] in their Q^2-scale change model proposed that the effective single nucleon structure functions in a nucleus (A) are related with that in deuteron by

$$F_2^A(x, Q^2) = F_2^D(x, \xi_A Q^2) \tag{16}$$

where ξ_A is a scale parameter weakly (logarithmically) dependence on Q^2. On the basis of bag model and QCD they further argued that ξ_A is related to r_A in nucleus by

$$\xi_A(Q^2) = (\frac{r_A}{r_N})^{2ln(Q^2/\Lambda^2)/ln(\mu^2/\Lambda^2)}. \tag{17}$$

By solving Eq.(15) we get the radius r_A for bound nucleon bag. There are three parameters r_N, G and α in Eq.(15) which can be determined through fitting the ξ_A values of five nuclei He, Be, Al, Fe and Au, which are obtained by rescaling experimental data; thus we get $r_N = 0.865$ fm, $G = 0.0362$ GeV fm, $\alpha = 0.541$. In calculation we used $\mu^2 = 0.63\ GeV^2$, $\Lambda = 0.250$ GeV. The results calculated for $Q^2 = 2.5\ GeV^2$ are summarized in Table II. The experimental values of ξ_A are not so definite. The difference between ξ_A–calculated calculated and ξ_A–experimental data for any nucleus A is around 5%.

Eq.(16) is a satisfying phenomenologically relation which all the data for different nucleus on l-A DIS process are in accordance with it.

Comparing the parameters $\xi_\alpha^A (\alpha = V, S, g)$ in Table I which comes from DQ^{2}RM with above the parameters ξ_A which describe the effect of QCD vacuum distortion in structure function of bound nucleon, we notice that:

1. Both the values of ξ_V^A in Table I and ξ^A (in Table II) are larger than unity and are weakly increasing as the nucleon number A increased.

2. For any nucleus (A fixed), ξ_V^A always larger than ξ^A, the differnece between them are essentially unvaried with A.

Furthermore, after taking the ξ_V^A and ξ_S^A from Table I and using the PDF of leading order of GRV parametrization, from Eq.(3) we get $F_2^A(x, Q^2)$ for various nucleus. Use Eq.(16) once more we get again the Q^2-rescaling parameters $\xi^A_{DQ^2RM}$ for structure functions of bound nucleon from DQ^{2}RM. We find for any nucleons, the difference between $\xi^A_{DQ^2RM}$ with ξ^A in Table II are less than 5%. This is just because both the parameter ξ_S^A and ξ_g^A in DQ^{2}RM are less than unity and they are decreasing as A increased, as seen in Table I.

Thus completed our demonstration for the DQ^{2}RM in high x-region.

IV. DEMONSTRATION FOR DQ^{2}RM IN LOW X-REGION

From any phenomenologically parameterization scheme for PDF of a nucleon we know that in low x-region, e.g. $x \leq 10^{-3}$ or even smaller, the distribution function of valence quark almost equal zero whereas that of the gluon and sea quark are increased very rapidly with the decrease of x; in addition the distribution function of gluon will nearly be 3 to 5 times as that of sea quark so as first approximation we will neglect their contributions.

In discussion of high energy γ^*-N(A) DIS process at low x-region, it seems more intuitive and convenient to use the space–time description approach in target rest frame, $\vec{P}_{N(A)} = 0$, rather than as usually use the Feynman-Bjorken infinite momentum $\vec{P}_{N(A)} \to \infty$ approach. In $\vec{P}_{N(A)} = 0$ frame, the incoming virtual photon state γ^* at a given instant of time, can be expanded in terms of its (bare) Fock states [17]:

$$|\gamma^* >_{phys} = \psi_\gamma|\gamma^* > + \psi_{q\bar{q}}|q\bar{q} > + \psi_{q\bar{q},g}|q\bar{q}, g > + \cdots . \tag{18}$$

In target rest frame when the scattering energy W of the virtual photon is vary high and its virtuality Q^2 is rather large, we could know this from [18] and [19] that in the probability amplitude $\psi_{q\bar{q}}$ of decaying into a $q\bar{q}$ pair, there is a rather large component in which the longitudinal momentum fractions of the quark and antiquark are nearly equal and their transverse separation $r_t(r_t(q\bar{q})) \sim \mathcal{O}(\frac{1}{Q})$. After scattering off the target, its transverse expansion $\Delta r_\perp$ is very small, thus this $q\bar{q}$ pair could be treated approximatedly as a colour dipole in the interaction with nucleon (nucleus) target. In this case only those gluons which

comes from the target with transverse momentum $k_\perp \sim \mathcal{O}(Q)$ could probe and interact with this colour dipole, so now we can use perturbative QCD to discuss γ^*-N(A) DIS process.

Based on this physical observation, Levin *et. al.* [9] using the generalized Glauber (Mueller) [10] formula for QCD diffractive coherent multi-scattering discussed how to get the gluon distribution function of nucleus, $g^A(x,Q^2)$ from that of nucleon, $g^N(x,Q^2)$. Since it is relevant for our later discussion, we will first give a schematically description about their approach.

Since the PDF of nucleon are independence of the probe what we taken, in order to avoid complexity which comes from quark line loop in $\gamma^* - g$ fusion subprocess in γ^*-N(A) DIS, Levin *et al* supposed a virtual "gluon probe" $\mathcal{G}$, which in target rest frame has very high energy and a rather large virtuality Q^2. The probe $\mathcal{G}$ decays into a gluon pair GG with nearly equal longitudinal momentum fraction and their transverse separation $r_\perp$ is rather small. The kinematics of this approach shown in Fig.5. This pair interacts with a nucleon due to exchange of a gluon ladder diagram, where $l_\perp$ denotes transverse momentum of the gluon in the ladder attached to GG pair. The Bjorken variable $x = \frac{Q^2}{\hat{s}}$, where $\sqrt{\hat{s}} = W$ is the e.m. energy of incoming "gluon" $\mathcal{G}$. The change in $r_\perp$ during the passage of GG pair through the nucleus $\Delta r_\perp \propto R\frac{k_\perp}{E}$, where E denotes the energy of the pair in target rest system and R is the size of target, the transverse momentum $k_\perp \propto \frac{1}{r_\perp}$. It is easy shown when W (and hence E) is very high and $x \ll \frac{1}{2mR}$, one get $\Delta r_\perp \ll r_\perp$ and thus the condition for using Glauber (Mueller) approach in discussing the GG pair interaction with the nucleus is satisfied. Then as in [9] the gluon distribution function of nucleus is given by

$$xG_A(x,Q^2) = \frac{4}{\pi^2}\int\limits_x^1 \frac{dx'}{x'}\int\limits_{\frac{4}{Q^2}}^{\infty}\frac{dr_\perp^2}{r_\perp^4}\int\limits_0^\infty \frac{d^2k_\perp}{\pi}2\{1 - e^{-\frac{1}{2}\sigma_N^{GG}(x',r_\perp^2)S(b_\perp^2)}\}. \tag{19}$$

The term in curly brackets is the total cross section of the interaction of gluon pair GG with nucleus in the eikonal approach. In double logarithmic approximation (DLA) for perturbative QCD, the GG pair cross section with the nucleon $\sigma_{GG}(x,r_\perp^2)$ can be written (for $N_c = 3$) as [20]

$$\sigma_{GG}(x,r_\perp^2) = \frac{3\alpha_s(\frac{4}{r_\perp^2})}{4}\pi^2 r_\perp^2(xg_N(x,\frac{4}{r_\perp^2}). \tag{20}$$

The factor $\frac{1}{r_\perp^4}$ in Eq.(19) comes from the wave function of the GG pair in probe $\mathcal{G}$ and $S(b_\perp)$ is the nucleon profile function in nucleus (A) with impact parameter $b_\perp$ for $\mathcal{G}$-A eikonal scattering. Usually it takes Gaussian form:

$$S(b_\perp) = \frac{A}{\pi R_A^2} e^{-\frac{b_\perp^2}{R_A^2}}. \tag{21}$$

Putting Eqs.(20) and (21) into Eq.(19) and integrate over $b_\perp$ we obtain in DLA the gluon distribution of bound nucleon:

$$xg^A(x,Q^2) \equiv \frac{1}{A} xG^A(x,Q^2) = \frac{2R_A^2}{A\pi^2} \int_x^1 \frac{dx'}{x'} \int_{\frac{1}{Q^2}}^{\frac{1}{Q_0^2}} \frac{dr_\perp^2}{r_\perp^4} \{C + ln(k_G(x', r_\perp^2)) + E_1(k_G(x', r_\perp^2))\}, \tag{22}$$

where C is the Euler constant and E_1 is the exponential integral and

$$k_G(x, r_\perp^2) = \frac{3\alpha_s A \pi r_\perp^2}{2R_A^2} x g_N(x, \frac{1}{r_\perp^2}) \tag{23}$$

If Eq.(22) is expanded in small k_G, the first term will correspond to the usual DGLAP equations in small x region (Born approximation of Mueller formula) while the other terms coming from GG pair coherently multi-scattering with nucleus what will take into account the shadowing corrections.

For concrete comparison the $xg^A(x,Q^2)$ calculated, from Glauber (Mueller) approach with those from DQ^{2}RM , we put $Q_0^2 = 0.5$ GeV^2 in Eq.(22) and calculate the $xg^A(x,Q^2)$ in $2 \le Q^2 \le 4$ GeV^2, $10^{-4} \le x \le 10^{-3}$ [2]. In this kinematic region we introduce the quantity:

$$\Delta_g^A \equiv \quad \text{Max} \quad \{\frac{xg^A(x,Q^2) - xg^A_{DQ^2RM}(x,Q^2)}{xg^A(x,Q^2)}\}, \tag{24}$$
$$10^{-4} \le x \le 10^{-3}$$
$$2 \le Q^2 \le 4\ GeV^2$$

where $xg^A(x,Q^2)$ is calculated from Eq.(22), and $xg^A_{DQ^2RM}(x,Q^2)$ is deduced from Eq.(1) and Table I, both of their input gluon distribution functions are LO of GRV parameterization sets [11]. In addition, when we put the $g^A(x,Q^2)$ resulting from Eq.(22) into Eq.(1), we get another Q^2-rescaling parameter, $\bar{\xi}_g^A$, for gluon distribution function from Glauber (Mueller) approach and we can compare it with those from Table I.

---

[2]From the DLA condition which required for validity of Eq.(22), our Q^2-range seems too low, but from the available data at such small x-region we found its Q^2-range just so low or even lower. On the other hand from the fact of "precocious Q^2-scaling", which revealed experimentally what the Bjorken Q^2-scaling in γ^*-N DIS process arrived practically at much lower Q^2 values than those predicted by perturbative QCD, one may expected, as a first approximation, one could using Eq.(22) at such low Q^2-range to calculate $xg^A(x,Q^2)$

In Table III we list the Δ_g^A, ξ_g^A and $\bar{\xi}_g^A$ for some nuclei, from it we see the Δ_g^A values for all but H^1 and Be^9 nuclei[3] are less than 5% and all the gluon Q^2-rescaling parameters of DQ^{2}RM , ξ_g^A are all very close to those $\bar{\xi}_g^A$, calculated from Glauber (Mueller) approach. In addition both the $\bar{\xi}_g^A$ or ξ_g^A seems approach its saturation value, ≥ 0.7 as $A \geq 200$, this is related to the fact that in $10^{-4} \leq x \leq 10^{-3}$ region the coherent length of the GG pair, $l_{GG} \sim \frac{1}{mx} \approx 10^3 - 10^4$ fm are much large than radius of nuclei, $R_A \leq 10$ fm and R_A approch also its saturation value as $A \geq 200$, so the rescattering number of GG pair in nucleus also approach saturation.

Here we want to point out that we could not expect in a similar simple manner as above formalism —Glauber (Mueller) approach in DLA— getting good results from calculating the sea quark distribution function of bound nucleon, $xq_S^A(x, Q^2)$. In other words, we could not take enough account the effect of nuclear shadowing on sea quark distribution functions from equations like Eq.(19) since there are two points in this case:

1. in small x-region, e.g. $10^{-4} \leq x \leq 10^{-3}$ sea quark distribution functions in nucleon are only $\frac{1}{5}$ to $\frac{1}{3}$ of that of the gluon.

2. The relevant splitting function are $P_{gq}(x) = P_{g\bar{q}}(x) = \frac{4}{3}\frac{(1+(1+x)^2)}{x}$, $P_{gq}(x) = 6[\frac{x}{(1-x)_+} + \frac{1-x}{x} + x(1-x) + (\frac{11}{12} - \frac{N_f}{18})\delta(1-x)]$. at small x limit their ratio approach $\frac{4}{9}$.

These two factors would cause the corresponding power for sea quark in the exponential term in curly bracket smaller about one order of magnitude. Thus with this simple no mixing (between sea quark and gluon) approach the resulting effect of nuclear shadowing correction on sea quark is very weak and the resulting $xq_S^A(x, Q^2)$ would be incorrect.

V. CONCLUSION AND COMMENTS

We have adopted different approaches at different x-regions to demonstrate the DQ^{2}RM for PDF of bound nucleon. For high x-region, $0.1 \leq x \leq 0.7$ we used the distorted physical vacuum picture and the soliton bag model to justify the radius of a bound

[3]Notice Eq.(22) is not an evaluation equation but a formula for getting $xG^A(x, Q^2)$ of nucleus. In calculating $xg^A(x, Q^2)$ with Eq.(22), we have let the GRV parameterization set $g^N(x, Q^2)$ of nucleon as input. Since this input comes from phenomenology, it should have included effects of rescattering, thus in some sense, this calculating method have some double counting, but it is only important for nucleon and few light nuclei.

nucleon always larger than that of free one. This effect causes the soften of PDF in bound nucleon, which turns to the Q^2-rescaling behavior revealed phenomenologically on structure functions of bounding nucleon. We thus have demonstrated the validity of DQ^{2}RM in high x-region. For low x-region $10^{-4} \leq x \leq 10^{-3}$ according the formalism of Levin *et al* in Glauber (Mueller) coherently multi-scattering approach, we have shown the resultant gluon distribution function of bound nucleon, $xg^A(x, Q^2)$ agree very well with those from DQ^{2}RM . Thus the validity for this phenomenological model are demonstrated.

Of course, both the DQ^{2}RM on its own and all our demonstrations about it are far from perfect. We want to make following observations about it.

First, although our demonstrations for DQ^{2}RM are physically reasonable, but it is far from satisfactory. We could not over the whole x-region using the perturbative QCD strictly and systematically justified this model, instead we adopted different approaches for different x-region. In particular we could not give a clear and physical argument for middle x-region, $10^{-1} \leq x \leq 10^{-3}$, where the contributions for valance quark, sea quark and gluon are comparatively in l-A DIS processes.

Second, although the DQ^{2}RM reflected approximatedly the objective reality of PDF in bound nucleon, but it is still a sketchy model. Indeed, if we have a detailed investigation on this model with perturbative QCD, it is possible to find that these Q^2-rescaling parameters, $\xi_\alpha^A(\alpha = V, S, g)$, are actually not constants, but perhaps like logarithmic, weakly depend both on x and Q^2.

Last, a very seriously problem is how to evaluate the non-perturbative QCD effects exerted on bound nucleons causing by the environment of nucleus. We have explained in Sec.III the EMC effect with the vacuum distored model in nuclei is just an example, but such non-perturbative QCD effects would be active over the whole x-region on PDF of bound nucleon.

Obviously, to complete settle these problems from genetic QCD are very difficult.

Acknowledgements

This work was supported in part by the National Natural Science Foundation of China, the Doctoral Program of Institution of Higher Education of China and the Natural Science Foundation of HeBei Province.

REFERENCES

[1] See, for example, M. Arneodo, Phys. Rep. **240**, 301(1994).

[2] J.J. Aubert, *et al*, Phys. Lett. **B123**, 275(1983).
A. Bodek *et al*, Phys. Rev. Lett. **50**, 1431(1983); **51**, 534(1983).

[3] P. Amaudruz *et al*, Z. Phys. **51**, 387(1991); J. Ashman *et al*, Phys. Lett. **B202**, 603(1988).

[4] R.L. Jaffe, Phys. Rev. Lett. **50**, 228(1983).
F.E. Close, R.G. Roberts and G.G. Rose, Phys. Lett. **B129**, 43(1983).

[5] J. Qiu, Nucl. Phys. **B291**, 746(1987).
E.L. Berger and J. Qiu, Phys. Lett. **B206**, 141(1988).
F.E. Close and R.G. Roberts, Phys. Lett. **B213**, 91(1989).
W. Zhu and J.G. Shen, Phys. Lett. **B219**, 107(1989); Phys. Lett. **B235**, 170(1990).

[6] Z. M. He, *et al*, Euro. Phys. J. **C4**, 301(1998).

[7] T.D. Lee, Particle Physics and Introduction to Field Theory, Harwood Acad. Pub., N.Y., 1981.

[8] H.A. Peng, *et al*, Chinese Phys. Lett. **2**, 65(1984).
L.S. Liu, H.A. Peng and W.Q. Zhao, Scientia Sinica **A28**, 1184(1995).

[9] A.L. Ayala, F.M.B. Gay Ducati and E.M. Levin, Proc. of the Workshop on Future Physics at HERA 1995/96, p.927; CBPF-FN-020/96, hep-ph/9604383, April 1996.

[10] A.H. Mueller, Nucl. Phys. **B335**, 115(1990).

[11] M. Glück, E. Reya and A. Vogt, Z. Phys. **C53**, 651 (1995); **C67**, 433 (1995).

[12] P. Amaudruz, *et al*, Nucl. Phys. **B441**, 3(1995).

[13] D.M. Alde *et al*, Phys. Rev. Lett. **64**, 2479(1990); **66**, 2285(1991).
M.R. Adems, *et al*, Phys. Lett. **B287**, 375(1992).

[14] P. Amaudruz, *et al*, Nucl. Phys. **B371**, 553(1992).

[15] G.L. Li, Z.J. Cao and C.S. Zhong, Nucl. Phys. **A509**, 757(1990).

[16] See, for example: F.E. Close, An Introduction to Quarks and Partons, 1997 Academic Press Inc..

[17] See, for example: P. Hoyer, "Interactions on Nuclei" in Workshop on DIS and QCD, Paris, 1995, edited by J.-F. Laporte and Y. Sirois.

[18] B.L. Ioffe, Phys. Lett. **30**, 123(1968).

[19] L. Frankfurt, W. Koepf and M. Strikmann, DESY 97-028, hep-ph/9702216.

[20] S.J. Brodsky *et al*, Phys. Rev. **D50**, 3134(1994).

TABLES

TABLE I. The fitted values of rescaling parameters.

	C^{12}	Ca^{40}	Fe^{56}	Sn^{119}
ξ_V	1.03	1.35	1.14	1.49
ξ_S	0.70	0.67	0.62	0.60
ξ_G	0.86	0.81	0.76	0.74

TABLE II. ξ_A and r_A/r_N for various nucleus.

Nucleus	ξ_A	r_A/r_N
He^4	1.223	1.065
Be^9	1.242	1.070
C^{12}	1.248	1.072
A^{27}	1.299	1.085
Ca^{40}	1.319	1.091
Fe^{56}	1.352	1.099
Ag^{107}	1.410	1.114
Au^{197}	1.696	1.180

TABLE III. A list of Δ_g^A, ξ_g^A and $\bar{\xi}_g^A$ for various nucleus.

A	H^1	Be^9	C^{12}	Al^{27}	Ca^{40}	Fe^{56}	Cu^64	Sn^{119}	Ze^{131}	Au^{17}	Pb^{208}
$\Delta_g^A(\%)$	12	9	4	5	4	1	2	1	1	1	1
$\bar{\xi}_g^A$	1	0.9	0.87	0.84	0.82	0.78	0.76	0.74	0.73	0.72	0.72
ξ_g^A	1		0.86		0.81	0.76		0.74			

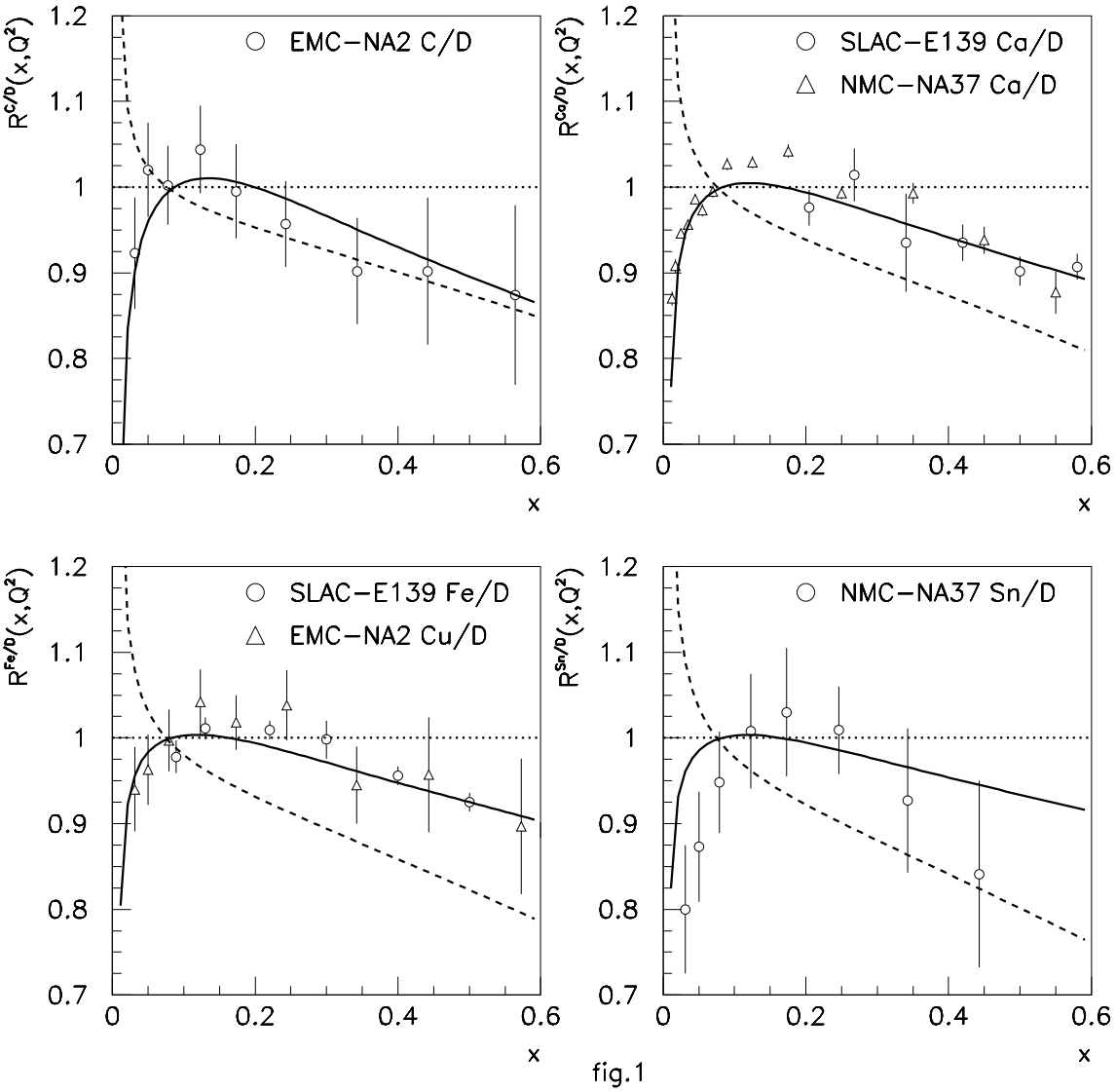

FIG. 1. The ratio $R^{A/D}(x,Q^2)$ for nuclei C^{12}, Ca^{40}, Fe^{56}, Sn^{119} versus the momentum fraction x with the corresponding experimental data [3,12]. The solid lines are the results of our model, the dashed lines are the results of the old Q^2-rescaling model in ref. [15].

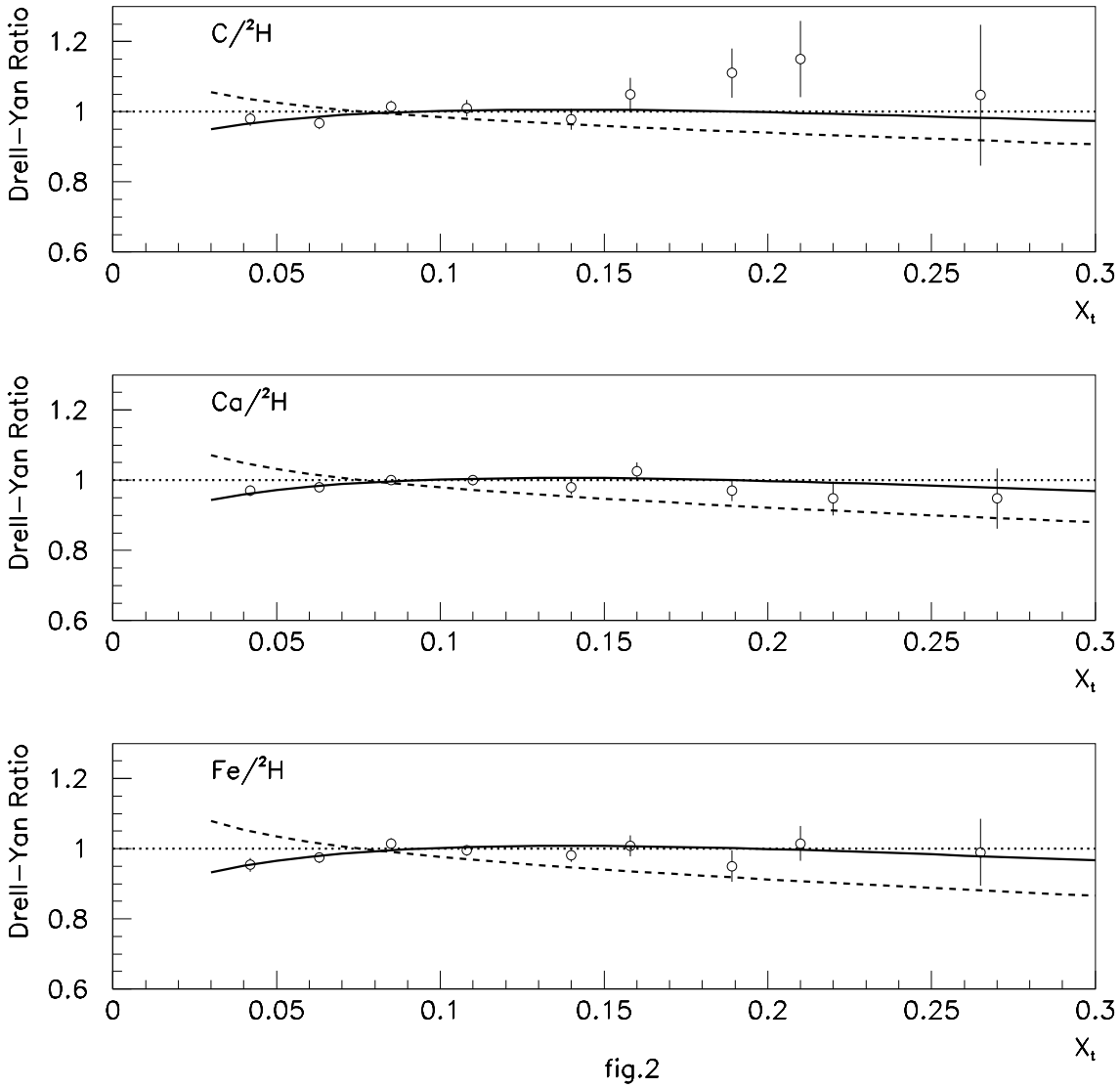

fig.2

FIG. 2. The ratio $T^{A/D}(x_t, Q^2)$ for nuclei C^{12}, Ca^{40} and Fe^{56} versus x within region of $0.025 \leq x_t \leq 0.30$, $4 \leq M_{l\bar{l}} \leq 9GeV$ and $E_{CM} = 40GeV$, where corresponding experimental data [13]are shown. The meaning of lines is the same as that in Fig.1.

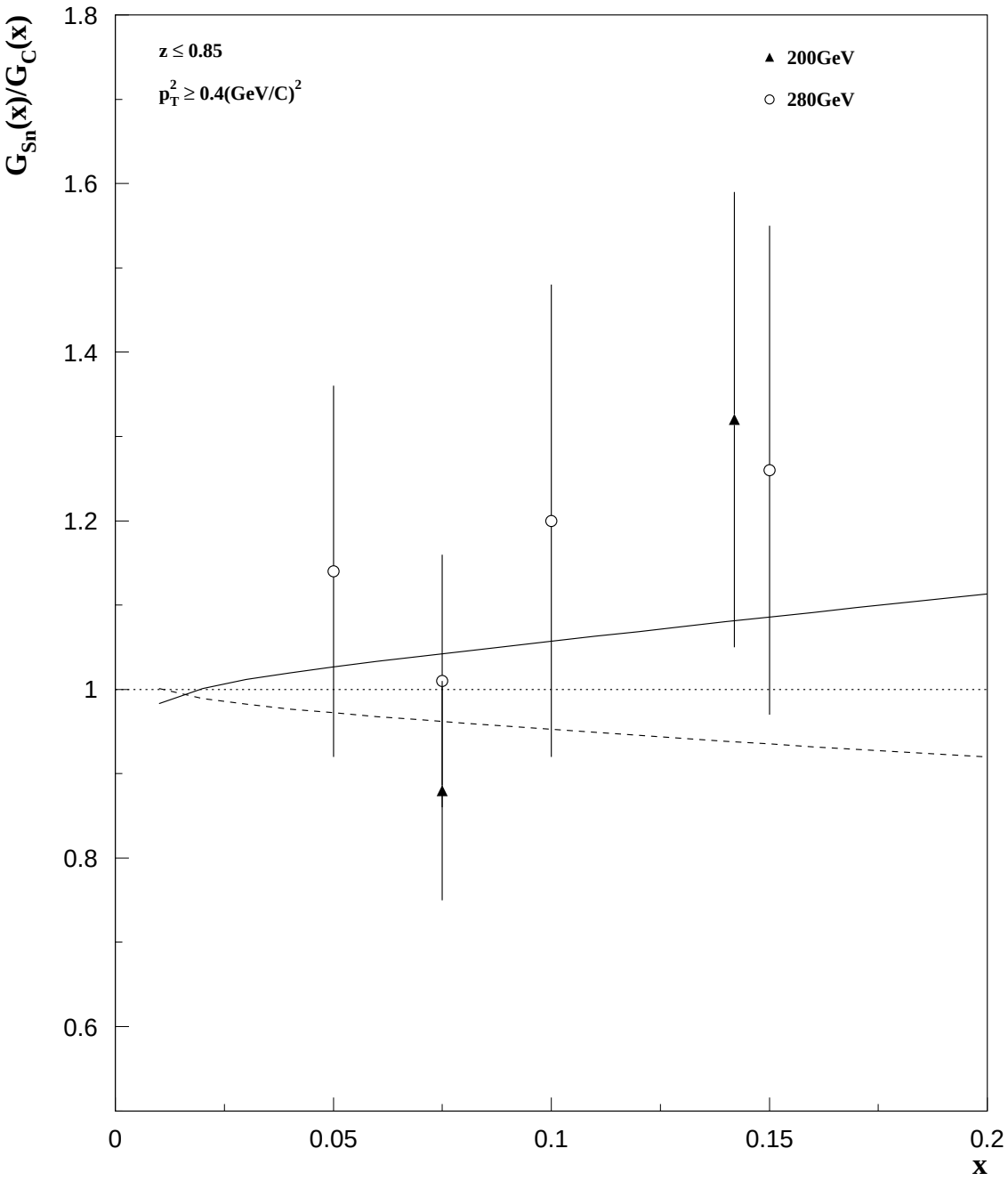

fig.3

FIG. 3. The ratio $R_G^{Sn/C}(x, Q^2)$ versus x, where the experimental data [14]are shown. The meaning of lines is the same as that in Fig.1.

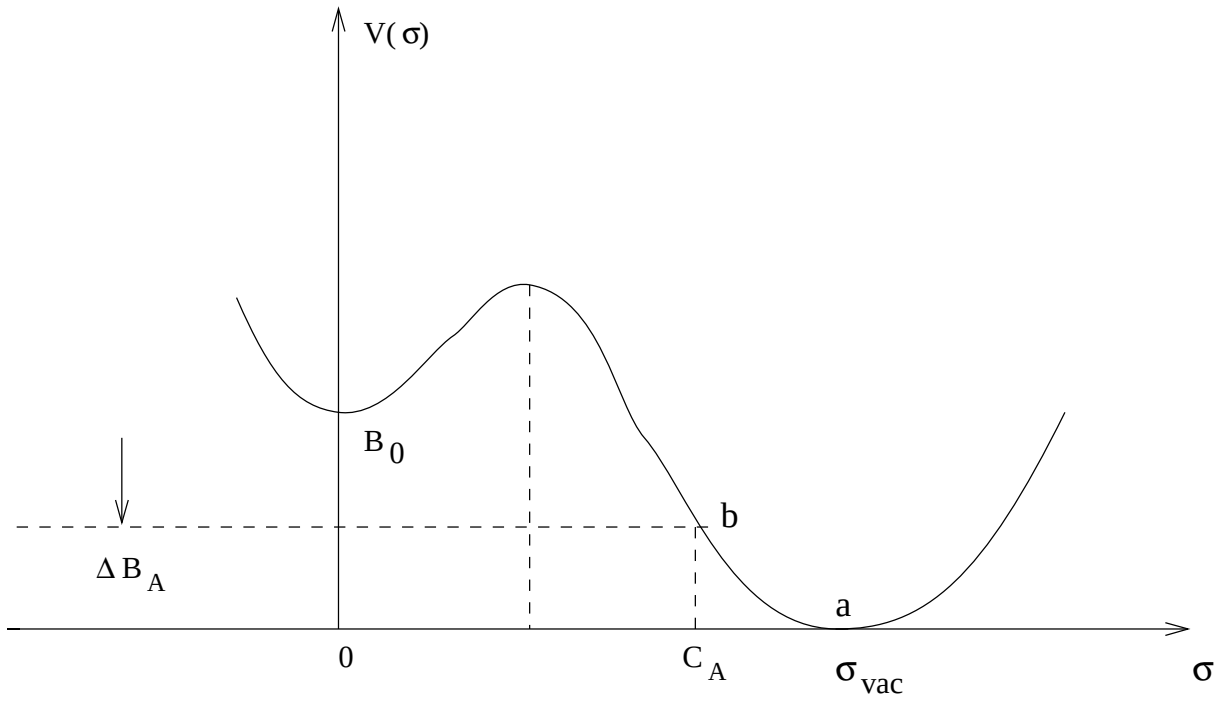

FIG. 4. The potential energy of σ-field and the change of the bag constant due to the change of σ-field in the vacuum.

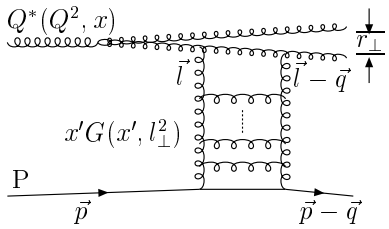

FIG. 5. Kinematics of the Glauber approach [9].